# Imaging Radar Sensor Front-End with a Large Transmit Array


Winfried Mayer[1], Stefan Buntz[2], Helmut Leier[2], Wolfgang Menzel[1]

[1]University of Ulm, Microwave Techniques, Albert-Einstein-Allee 41, 89081 Ulm, Germany,
Phone ++49 731 5026360, winfried.mayer@ieee.org
[2]DaimlerChrysler AG, Research & Technology, Wilhelm-Runge-Strasse 11, 89013 Ulm, Germany



***Abstract*— A 24 GHz imaging radar front-end intended for medium range automotive applications is presented in this article. In the front-end a large switched transmit antenna array is combined with a coherent FM-CW architecture. It allows two dimensional electronic scanning in range and cross range with good cross range resolution over a wide angle of view using very low EIRP. In comparison to complex and cost intensive phased array approaches, it requires only a moderate number of active millimeter wave components. Within the scope of this paper an overview of the front-end's architecture, design and realization is given. Performance is demonstrated by exemplary radar images obtained from measurements with a first setup.**


## I. Introduction

In the application fields of automotive sensors, features like parking aid, closing velocity sensing (precrash), line prediction, and stop-and-go are to be addressed by short and medium range radars [1]. The key requirements for these sensors are good cross range resolution and a large field of view. These requirements should be met by low cost sensors hidden behind the bumper of a car. Arrays of four to six simple pulsed range sensors equally spaced across the front bumper of a car are one present approach, which is close to series production [2]. Cross range resolution is obtained with the sensor array by means of multilateration [3], [4] or monopulse [5]. With high bandwidth [6] both principles are advantageously for parking aid as they are providing good two-dimensional resolution at very short ranges. However, their cross range resolution is depending on the range resolution and, with respect to multilateration, decreasing with range. In the approach presented here, cross range information is obtained from scanning the sensor's aperture, and range information is obtained by frequency modulation. So range and angular resolution are independent from each other.

To achieve electronic cross range scanning with a minimum of RF hardware the front-end uses switches to access a series of linearly arranged antenna elements with one transmitter stage. Cross range information is obtained synthetically by signal processing of the successively recorded one-dimensional range scans for all antenna elements. Compared to other switched approaches [7], [8] only the transmit and not the receive paths are switched. So receiver noise figure is not affected by the insertion loss of the switches.

The sensor front-end is designed primarily to address automotive medium range applications up to 40 m [1] with the perspective of combining medium and long range applications in one sensor.

## II. Front-End Architecture

A switched principle has been chosen taking into account available microwave integrated circuits, maximum acceptable dimensions, a maximum field of view in cross range and noise and tolerance aspects. Fig. 1 illustrates the functional block diagram of the front-end. The antenna is consisting of 25 switched transmit elements and two non switched receive elements left and right to the transmit array. All antenna elements are linearly arranged and equally spaced with half a wavelength distance at minimum RF frequency.

Ramped or triangular RF waveforms are passed by a switching network (SP25T) to one of the 25 transmit antennas (TX1-TX25). Reflected signals are received in parallel by two receive blocks. The receive blocks include a low noise amplifier (LNA), a down-converter (MXR), an intermediate frequency (IF) stage and an analog to digital converter (A2D). The local oscillator signals for the mixers are coupled out from the transmit waveform. The synthetic cross range processing requires signal coherence during the whole scanning sequence and modulation waveforms with defined slopes and good frequency linearity. These requirements are met by a combination of a direct digital synthesizer (DDS), a phase locked loop (PLL) and a frequency multiplier (MULT) [9].

If, in a basic operation mode, FM-CW radar scans with identical ramped waveforms are executed for all receive-transmit combinations, a two dimensional radar image for position vectors $\vec{r} = \vec{r}(R, \theta)$ can be obtained by phase correction and coherent integration of the sampled and stored data according to equation (1). Combining the transmit scans for the two receive channels to a synthetic aperture similar to [10], [7], cross range resolution can be increased to a value that would normally require a real aperture of twice the front-end's width. With this synthetic aperture and applying far field approximations equation (1) can be simplified to (2) representing two cascaded discrete Fourier transforms and one phase shifting term. To emphasize the Fourier transforms the substitutions $u = \frac{f_0}{c_0} \cdot d \cdot \sin(\theta)$ for the angular coordinate and $v = \frac{S}{c_0} \cdot t_s \cdot R$ for the range coordinate are introduced in (2). The phase shifting term is accounting for the hardware related phase differences of the $l'$ transmit

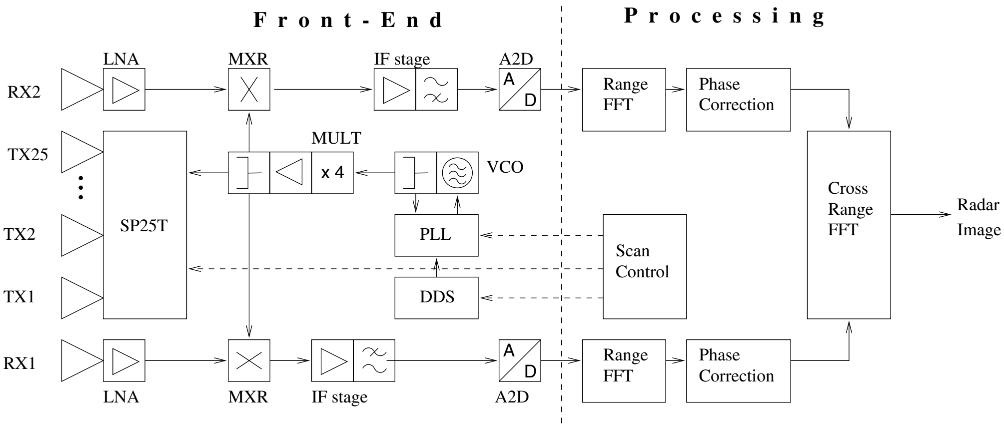


Fig. 1. Functional block diagram of the sensor front-end.

receive combinations of the synthetic array. With the prerequisite of equally spaced elements and accepting non equally spaced angular samples, processing of (2) can be performed by fast Fourier transform algorithms leading to short processing times.

$$A(\vec{r}) = \sum_{m=1}^{2}\sum_{l=1}^{n_{\mathrm{tx}}}\sum_{i=1}^{n_{\mathrm{s}}} a_s(m,l,i) \quad (1)$$

$$\cdot \mathrm{e}^{-\mathrm{j}\frac{2\pi}{c_0}(f_0+St_s i)\cdot|\vec{r}_{\mathrm{rx}}(m)+\vec{r}_{\mathrm{tx}}(l)-2\vec{r}|} \cdot \mathrm{e}^{-j(\phi_{\mathrm{tx}}(l)+\phi_{\mathrm{rx}}(m))}$$

with

| | | |
|---|---|---|
| $a_{\mathrm{s}}(m,l,i)$ | = | recorded samples |
| $n_{\mathrm{tx}}$ | = | number of transmit elements |
| $n_{\mathrm{s}}$ | = | number of samples per waveform |
| $t_{\mathrm{s}}$ | = | sampling time |
| $S$ | = | frequency slope of ramped waveform |
| $f_0$ | = | start frequency |
| $c_0$ | = | speed of light |
| $\vec{r}_{\mathrm{tx}}(l), \vec{r}_{\mathrm{rx}}(m)$ | = | position vector of $l^{\mathrm{th}}$ transmit and $m^{\mathrm{th}}$ receive element |
| $\phi_{\mathrm{tx}}(l), \phi_{\mathrm{rx}}(m)$ | = | phase correction value of $l^{\mathrm{th}}$ transmit and $m^{\mathrm{th}}$ receive element |

$$A(v,u)=\sum_{l'=-n_{\mathrm{tx}}}^{+n_{\mathrm{tx}}}\left(\sum_{i=1}^{n_{\mathrm{s}}} a_{\mathrm{s}}\cdot \mathrm{e}^{-j2\pi vi}\right)\cdot\mathrm{e}^{-j\phi(l')}\cdot\mathrm{e}^{-j2\pi ul'} \quad (2)$$

At present the basic signal processing blocks are fast Fourier transforms in range and cross range which are applied to the sampled and stored receive signals from all the receive-transmit combinations. Kaiser or Taylor window functions are used to reduce the side lobes of the angular target response. In between the two Fourier transform steps, phase and amplitude differences of the switched transmit paths and the two receive paths, are compensated with appropriate correction vectors. For the application of the window functions it is necessary to interpolate the amplitude of the missing element combination for $l' = 0$ to get satisfactory side lobe suppression. The signal processing method described just now is only the basic example out of many possibilities to calculate radar images from data recorded with the presented front-end. As the setup allows versatile transmit waveforms and scanning sequences, various signal processing techniques can be examined with respect to the specific automotive fields of application.

## III. Design and Realization

All active RF blocks are realized by commercially available standard MMICs. The switching network is realized with commercially available 6-port MMIC switches [11], which are based on pin diode pairs. Transmit and receive antennas are a three element series patch design. They are linearly arranged with equal spacing of half a wavelength and are realized on one common substrate. The switches and the LNAs are integrated together with appendant electronics in a multi-layer board consisting of one RF substrate and two epoxy substrates and providing 4 metal routing layers. All millimeter wave circuitry is realized in microstrip technique on the RF substrate. The antenna substrate is mounted on top of the multi-layer board. For flexibility reasons of the first setup, further building blocks have been realized as separately housed coaxial elements. However they are planned to be integrated in the multi-layer very soon to demonstrate a compact front end design.

As the transmission line lengths to the individual transmit antennas are not equal, their different phases are compensated in the signal processing by multiplication after the Fourier transform in range. The phase compensation vector thereto had to be found by measurements, as assembly tolerances in the contacting of the MMICs made it impossible to use the values predicted by simulation. In Fig. 2 a comparison between measured and simulated relative phases of the 25 transmit elements is shown. The good agreement between the measurements in far-field and near-field indicates, that despite their narrow spacing of only 6 mm, parasitic radiation by neighboring elements is very low.

Fig. 3 is a photograph of the frontal view of the sensor front-end with the radome removed. Visible are the antenna array, the switch arrangement and the LNAs. The front-end's cross section dimensions are 175 mm and 58 mm.

## IV. Radar Measurement Results

With the sensor front-end of Fig. 3 and further external building blocks, a first demonstration sensor setup has

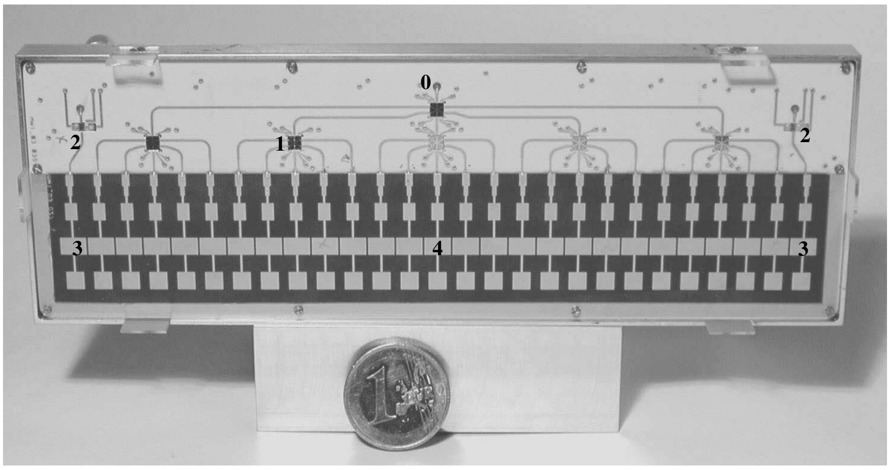

Fig. 3. Frontal view of the sensor front-end with the radome removed. Indicated are one of the six transmit MMIC switches 1, the two receive LNAs 2, the receive antenna elements 3, the center transmit antenna element 4 and the coaxial feed for the transmit signal fed from backside 0.

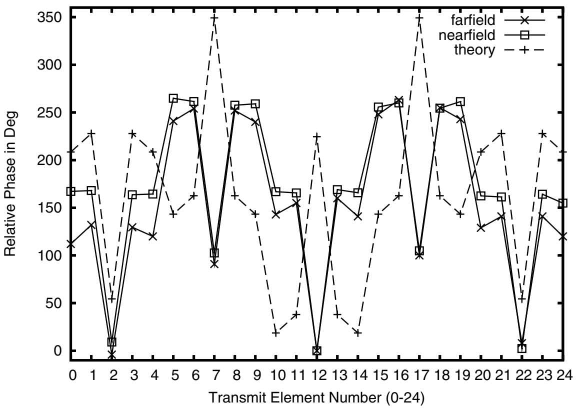


Fig. 2. Measured and simulated phase compensation vectors of the 25 transmit elements at a frequency of 24 GHz.

been composed and successfully tested. An exemplary radar image with ideal and real targets is shown in Fig. 4 in a perspective surface plot. The corresponding scenery is included in the pseudo-color plot of the same image in Fig. 5. The image has been recorded using ramped waveforms with sweep times of 450 µs and a frequency deviation of 1.1 GHz. Transmit power was less than 5 dBm EIRP, and the picture is derived from one scan of all transmit antennas (no integration or averaging of images). The two receiver arrangement is used to improve cross range resolution as explained in paragraph II. From measurements of ideal metal post targets, a cross range resolution of 2.8° is found which is in good agreement with theory. Fig. 5 demonstrates that metal targets like cars and posts can be detected and located in two dimensions with close to 20 dB target dynamic range. As reflections of persons are an order of magnitudes lower, they have similar levels than cross range side lobes from strong targets like cars. Due to unsymmetries in the radiation diagrams of the individual antenna elements, the application of window functions to reduce cross range side-lobes is not yet as effective as predicted by simulations.

In Fig. 6 the radar image of a medium range measurement is presented. Various post targets and a car can be identified with target dynamic ranges between 10 dB and

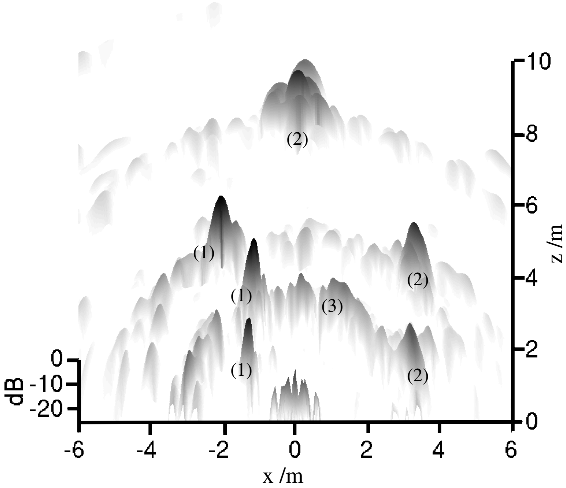


Fig. 4. Exemplary radar image in a three dimensional perspective plot with intensity coded amplitudes in dB. Target power dynamic range is from -25 dB (white) to 0 dB (black) nomalized to the maximum target. The identified target responses are three metal posts with 10 cm diameter and 1.5 m length (1), two small size cars (2) and a person (3). Sensor position is at $x = z = 0$.

20 dB in a realistic road scenery. The image is recorded with frequency ramps of 900 µs ramp time and 550 MHz deviation. The picture is calculated from one scan with a net recording time of $n_{\text{tx}} \cdot t_{\text{s}} \cdot n_{\text{s}} = 25 \cdot 900\,\mu\text{s} = 22.5\,\text{ms}$.

## V. Conclusion

A 24 GHz short range imaging radar front-end for automotive applications has been introduced and an overview on its architecture, design and realization has been given. Performance of the sensor idea has been demonstrated by an exemplary radar image of a realistic scenery recorded with a first sensor setup. In the near future the setup will be supplemented by a real time data acquisition, to be able to investigate the sensor idea for moving targets. Ongoing discussion on frequency standards for automotive radar brought up the question on transferring the front-end-architecture to higher frequencies (e. g. 77 GHz). Although this would require more precise

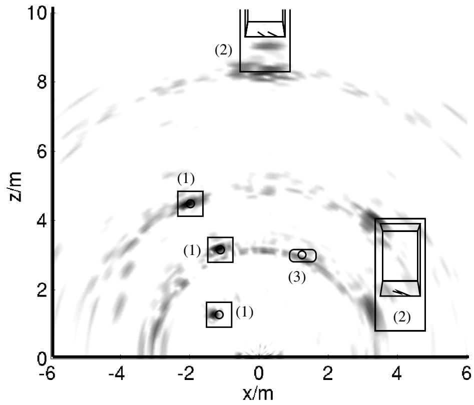


Fig. 5. Pseudo-color plot of the radar image of Fig. 4 with symbols of the corresponding scenery. Target power dynamic range is again from -25 dB (white) to 0 dB (black) nomalized to the maximum target. The identified targets are numbered as in Fig. 4.

assembly technologies, the architecture's advantages of electronic scanning with a minimum amount of active millimeter wave components and moderate sensitivity against tolerances in the RF circuitry would be advantageous, too.

## REFERENCES


[1] R. Mende and H. Rohling, "New automotive applications for smart radar systems," in *German Radar Symposium (GRS) Proceedings*. DGON, September 2002, pp. 35–40.

[2] J. Wenger and R. Schneider, "Automotive radar sensors," in *IEEE MTT-S Int. Microwave Symposium (IMS), Automotive Radar Workshop*, June 2002.

[3] M. Klotz, "An automotive short range high resolution pulse radar network," Ph.D. dissertation, University of Hamburg-Harburg, Jan. 2002.

[4] B. Michael and W. Menzel, "A realtime close-range imaging system with fixed antennas," in *IEEE MTT-S Int. Microwave Symposium (IMS) Digest*, 2000.

[5] M. Schneider, V. Gross, O. Brüggemann, T. Focke, T. Hansen, J. Schöbel, and T. Schöberl, "Automotive 24 GHz short range radar (srr) sensors with smart antennas," in *German Radar Symposium (GRS) Proceedings*. DGON, September 2002.

[6] I. Gresham, A. Jenkins, R. Egri, C. Eswarappa, F. Kolak, R. Wohlert, J. Bennett, and J.-P. Lanteri, "Ultra wide band 24 GHz automotive radar front-end," in *IEEE MTT-S Int. Microwave Symposium (IMS) Digest*, vol. 1, June 2003, pp. 369–372.

[7] Y. Asano, "Millimeter-wave holographic radar for automotive applications," in *European Microwave Conference (EuMC)*, 2001.

[8] C. Metz, J. Grubert, J. Heyen, A. F. Jacob, S. Janot, E. Lissel, G. Oberschmidt, and L. C. Stange, "Fully integrated automotive radar sensor with versatile resolution," *IEEE Transactions on Microwave Theory and Techniques*, vol. 49, no. 12, pp. 2560–2566, December 2001.

[9] W. Mayer, M. Wetzel, and W. Menzel, "A novel direct-imaging radar sensor with frequency scanned antenna," in *IEEE MTT-S Int. Microwave Symposium (IMS) Digest*, vol. 3, no. 9, 2003, pp. 1941–1944.

[10] N. Kees, E. Schmidhammer, and J. Detlefsen, "Improvement of angular resolution of an millimeterwave imaging system by transmitter location multiplexing," in *IEEE MTT-S Int. Microwave Symposium (IMS) Digest*, 1995, pp. 969–972.

[11] *23–26 GHz GaAs MMIC 6 Port Reflective PIN Switch*, Skyworks, December 2002.


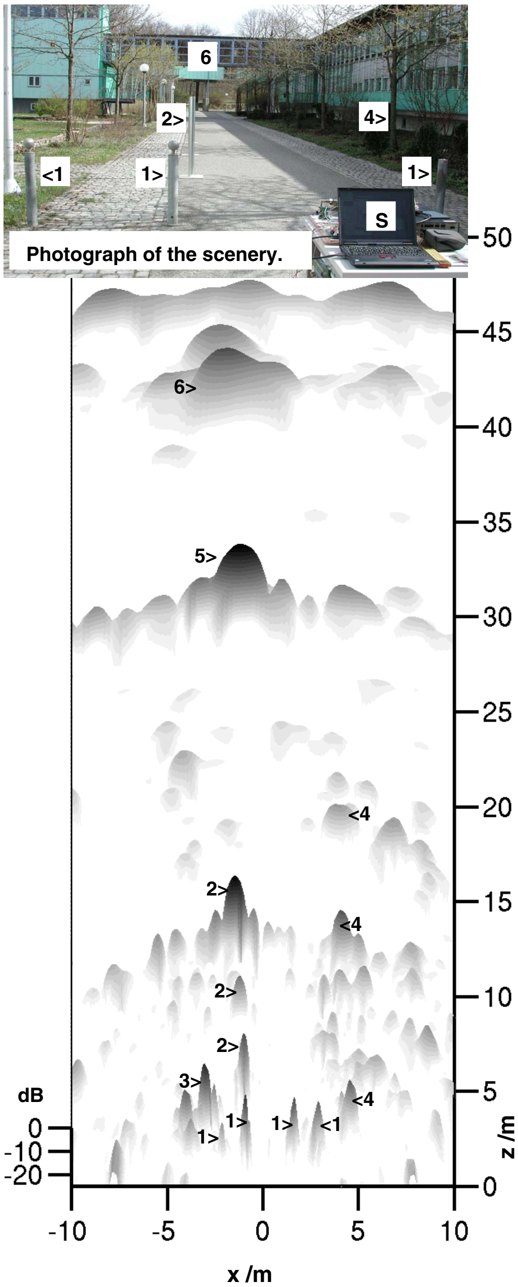


Fig. 6. Road scenery as an example of a medium range radar image in a perspective plot. Identifiable targets are marked with numbers: 1 a horizontal row of 4 metal posts with diameters of 8 cm and heights of about 80 cm, 2 three metal posts with 10 cm diameter and 1.5 m hight aligned along the z-axis, 3 a lamp post, 4 some trees, 5 a car at a distance of $z = 32$ m and 6 a skyway crossing the road at a distance of about 45 m. Target power dynamic range is from -30 dB (white) to 0 dB (black) normalized to the maxim target. Some of the targets and the sensor S are depicted in the photograph of the scenery on top of the radar image. The car 5 is not visible on the photograph.